Creation of self-assembled mesoscale chainmail and application

DATTA, Sougata

2,200,000

[2]

Efficient surface-catalyzed heterogeneous nucleation combined with nanospace engineering in toroidal molecular assembly enables precise control over the synthesis of self-assembled catenated materials. This research project undoubtedly paves new avenues for exploring advanced mesoscale materials.

In this study, we developed a unique methodology to control the catenation tendency for self-assembled toroidal nanoaggregates of barbituric acid molecules by tuning the inner void space of nanotoroids and the frequency of secondary nucleation. A reduction in the inner diameter of the nanotoroids results in nano-[2]catenanes in a high yield due to enhanced secondary nucleation and subsequent steric suppression of further catenation. Furthermore, we demonstrated the influence of seed topologies on seeded supramolecular polymerization by studying distinct kinetics of secondary nucleation and elongation using unique open- and close-ended seeds. These results will provide new molecular design guidelines for developing mesoscale functional materials.

Supramolecular polymer

Supramolecular polymer Nanotoroid barbiturate secondary nucleation catenane

１．研究開始当初の背景

Catenanes represent a major class of mechanically interlocked molecular ensembles comprising two or more mechanically bonded macrocyclic molecules that are spatially associated without being bonded together. Poly[n]catenanes are their corresponding polymeric or oligomeric versions composed of a large number of interlocked rings. These molecules endow the material with the dynamic properties associated with the high degrees of freedom in the motion of their constituent rings. The characterization of main chain poly[n]catenanes composed of large and flexible macrocycles is challenging because their crystallization is extremely difficult. We reported the preparation of nano-polycatenanes by kinetically organizing a barbituric acid-based small molecule into toroidal supramolecular polymers (*Nature* **2020**, *583*, 400). The nanoscale dimension of the toroidal building blocks enabled easy characterization of their mechanically interlocked bonding by microscopic technique.

２．研究の目的

Barbituric acid molecule **1**, featuring a diphenylnaphthalene moiety and terminal dodecyl chains forms a hydrogen-bonded hexamer called "rosettes", and can hierarchically organize into various structures depending on the assembly conditions (Figure 1a-c). For example, slow cooling of a hot monomeric solution of **1** forms helicoidal structures via thermodynamically controlled supramolecular polymerization. Conversely, fast cooling yields toroids as kinetically trapped species. These results suggested spontaneous generation of curvature in the supramolecular polymerization of **1** because rosettes continuously stack with rotational and translational displacements. Interestingly, by employing a solvent-mixing protocol that allows a more inhomogeneous kinetic aggregation, **1** furnished self-assembled catenanes (Figure 1d).
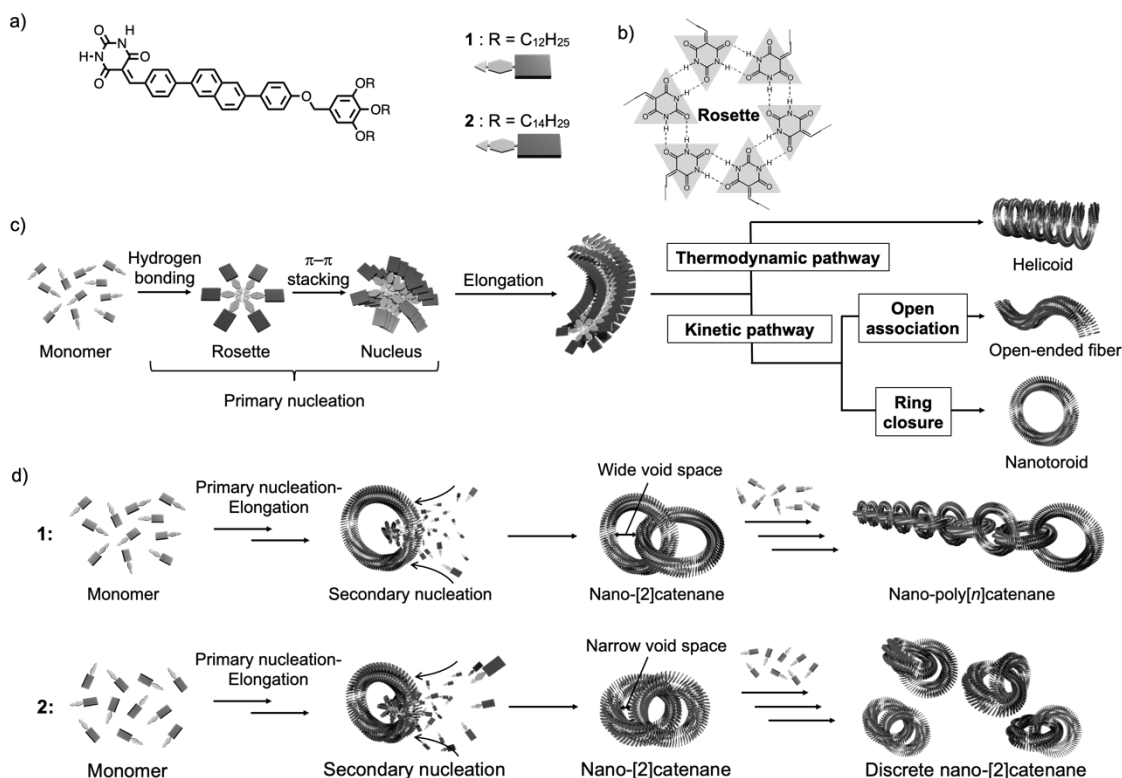

Figure 1. a,b) Molecular structures of **1** and **2**, and illustration of a hydrogen-bonded cyclic hexamer (rosette). c) Schematic representation of the primary nucleation of barbiturate monomers leading to various topological supramolecular polymers through thermodynamically and kinetically controlled supramolecular polymerization. d) Schematic representation of secondary nucleation on the inner surface of **1** and **2** nanotoroids, leading to different nano-catenane species.

Based on the mechanistic analogy with Sauvage's template-directed synthesis of molecular catenanes, the catenation of our nanotoroids could be attributed to secondary nucleation, i.e., surface-catalyzed heterogeneous nucleation of coexisting molecules on the surface of toroids. Once nano-[2]catenane formed, it elongated further into oligo and poly[*n*]catenanes owing to enhanced intermolecular interactions in the specific nanospace provided by two interlocked toroids that facilitate secondary nucleation more effectively than the single toroids.

Stimulated by these results, we aimed to prepare a chainmail-like 2D catenated structure. Since the secondary nucleation occurs uniformly on the surface of the nanotoroids, catenation proceeds in an uncontrolled fashion. Toward our goal, we tackled several challenges including modulation of the size of the void of the nanotoroids, controlling the secondary nucleation on the surface of the nanotoroids, and distinct kinetic studies of terminal elongation and secondary nucleation-elongation.

３．研究の方法

Nuclear magnetic resonance (NMR) spectroscopy, electrospray ionization mass (ESI-MS)

^{1}H and ^{13}C spectra were recorded on Bruker DPX 300 spectrometer and JEOL JMN-ECA500 NMR spectrometer. ESI-MS and APCI-MS spectra measurements were conducted on Thermo Scientific Exactive.

Atomic force microscopy (AFM)

AFM imaging was carried out under ambient conditions using Multimode 8 Nanoscope V (Bruker) in Peak Force Tapping (ScanAsyst) mode. Silicon cantilevers (SCANASYST-AIR) with a spring constant of 0.4 N/m and frequency of 70 kHz (nominal value, Bruker, Japan) were used. The samples were prepared by spin-coating (3000 rpm, 1 min) of solution (10 μL) of supramolecular polymers onto freshly cleaved highly oriented pyrolytic graphite (HOPG, 5 mm × 5 mm) at 293 K. Images were processed using NanoScope Analysis 3.00 (Bruker Instruments) and ImageJ v1.53s (National Institutes of Health).

Estimation of the relative area (%) of different topologies

One hundred 500 × 500 nm^2 AFM images for a particular sample were acquired using Multimode 8 Nanoscope V (Bruker Instrument) in Peak Force Tapping (Scanasyst) mode. The total number of single and interlocked toroids was counted for all the AFM images. The surface area of a single toroid and total surface area occupied by all the topologies were measured using the Bearing Analysis mode of a Nanoscope analysis software. The total surface area occupied by single toroids was calculated by multiplying the number of single toroids with the surface area of a single toroid, while the total surface area covered by catenanes was obtained by multiplying the number of interlocked toroids by the surface area of a single toroid. The relative surface area (%) of catenanes and single toroids were estimated with respect to the total area of catenanes, toroids, and random coil using the following equations.

Relative surface area of single toroids (%) = 100 × (Surface area of single toroids) / (Surface area occupied by all topologies)

Relative surface area of catenanes (%) = 100 × (Surface area of interlocked toroids) / (Surface area occupied by all topologies)

Relative surface area of random coil (%) = 100 − (Relative surface area of single and interlocked toroids)

UV-Vis spectroscopy and analysis of seeded supramolecular polymerization

UV-Vis absorption spectra were recorded on a JASCO V660 spectrophotometer equipped with a JASCO ETCS-761 temperature controller using a screw-capped quartz cuvette with an optical path length of 1 cm. Time-dependent changes in the molar fractions of aggregates, $\lambda_{(470\ nm)}$, at a certain temperature (T) in the presence and absence of toroid seeds was calculated from the absorption intensity at λ = 470 nm based on the following equation:

λ_{470} = [Abs$_{470}$(T) − Abs$_{470}$(*fully monomeric*)] / [Abs$_{470}$(*fully aggregated*) − Abs$_{470}$(*fully monomeric*)]

where Abs$_{470}$(T) is the absorption intensity at a given temperature (T), Abs$_{470}$(*fully monomeric*) and Abs$_{470}$(*fully aggregated*) are the absorbances of the purely monomeric state (at the highest temperature) and fully aggregated state (at the lowest temperature), respectively.

Preparation of self-assembled catenanes

100 μL of the chloroform (good solvent) solution (c_T = 1 × 10^{-3} M) of **1** or **2** taken in a Hamilton syringe (volume = 100 μL) was injected in ten portions (one 10 μL injection per second approximately) into 900 μL of MCH (poor solvent) taken in a glass vial at 293 K. The final concentration of the solution obtained after solvent mixing is 1 × 10^{-4} M.

Preparation of toroid solution

A monomeric solution of **1**, **2**, or **3** in chloroform (c = 1.0 × 10^{-3} M, 100 μL) was injected at once into 900 μL of MCH at r.t. The resulting solution was heated at 363 K (for **1** and **3**) and 353 K (for **2**), for 5 min and subsequently cooled to 293 K at a cooling rate of 1.0 K min^{-1}. The resulting solution was passed through a membrane filter of 200 nm pore size to filter out the elongated fibers from toroids.

Preparation of helicoid seed

A helicoidal supramolecular polymer solution was initially prepared by cooling a hot MCH solution of **2** (c = 1.0 × 10^{-5} M) from 373 K to 293 K at a cooling rate of 1.0 K min^{-1}. The helicoidal supramolecular polymer solution was sonicated for 15 s at 293 K to give a short helicoid solution.

４．研究成果

Controlled catenation of nanotoroids

We conducted research aimed at controlling of catenation of nanotoroids, which is essential for the creation of chainmail (*Chem. Sci.* 2023, *14*, 3270). The catenation relies on the size of the void of the nanotoroids and the secondary nucleation on their surface. Since the corresponding nanotoroids are covered with alkyl chains of the barbiturate monomer, we synthesized a new barbiturate **2** with longer tetradecyl chains to prepare nanotoroids with a larger void space and with higher efficiency of secondary nucleation on their surface (Figure 1a). AFM experiment revealed that **2** formed nano-[*n*]catenanes with higher yield than **1** (Figure 2a). However, analysis of the distribution of catenation number [*n*] revealed that **2** furnished a higher number of nano-[2]catenanes and a lesser number of oligomeric nano-[*n*]catenanes compared to **1** (Figure 2b-e). Spectroscopic studies of aggregation kinetics of the monomers showed a higher efficiency of secondary nucleation on the surface of nanotoroids of **2** than that of **1**. The longer alkyl chains of **2** enhanced the intermolecular interaction on the surface of toroids, which is favorable for surface-catalyzed secondary nucleation.

To find out why nano-[2]catenanes of **2** are less likely to elongate despite the higher efficiency of secondary nucleation of **2** than **1**, we measured the void size of the nanotoroids by AFM experiment. Strikingly, we found a smaller inner diameter (void size) of nanotoroids of **2** than that of **1** (Figure 2f,g). The smaller void size is not only because of the thicker diameter of the supramolecular fiber but also because of the tighter curvature formed by **2** than by **1**. This can be attributed to a larger rotational and translation slip of the rosettes of **2** compared to those of **1** upon stacking, as longer tetradecyl chains are sterically more demanding than dodecyl chains. Based on these results, we concluded that the steric factor associated with the lack of sufficient void space for generating additional supramolecular fibers through secondary nucleation reduces the tendency of nano-[2]catenanes of **2** to elongate further (Figure 1d). Accordingly, once the nano-[2]catenane was formed by **2**, it prevented the subsequent catenation due to a narrow void space.
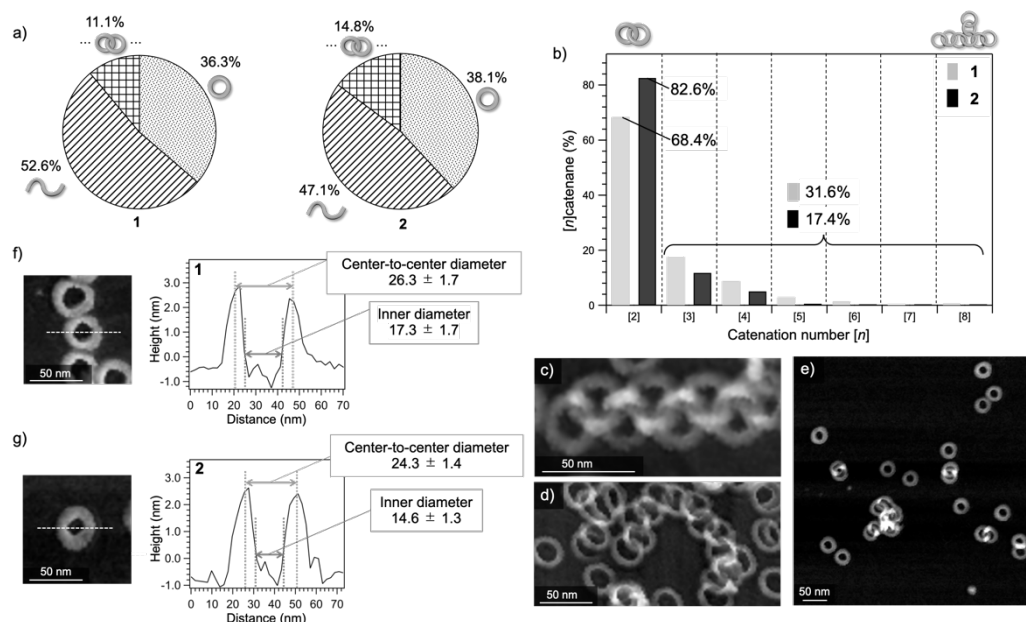
Figure 2. a) Pie charts showing the yields of catenanes, single toroids, and open-ended fibers of **1** and **2**. b) Bar charts showing the percentages of oligomeric nano-[*n*]catenanes (*n* = 2-8) of **1** and **2**. c-e) AFM images of nano-[*n*]catenanes formed by **1** (c,d) or **2** (e). f,g) AFM cross-sectional analysis for nanotoroids of **1** (f) and **2** (g) along the white lines.

Distinct kinetics of terminal elongation and secondary nucleation-elongation

We also compared the impact of terminal elongation and secondary nucleation-elongation in seeded supramolecular polymerization, which is crucial in studying the mechanism of mesoscale chainmail formation (*Chem. Commun.* **2023**, *59*, 7375). So far, we have studied secondary nucleation by performing seeding experiments just below the nucleation temperature, wherein spontaneous nucleation was delayed. Although toroid seed remained stable in this supersaturated condition, helicoid seed dissociated due to the presence of termini. Therefore, it is difficult to prepare a supersaturated solution of **1** wherein helicoid seed is stable. We rationally designed a new molecule **3**, having an electron-deficient quinoline unit (Figure 3a) that is expected to assemble weaker than **1**. As a result, its spontaneous nucleation was suppressed enough even under ambient conditions where both closed and open-ended seeds remained intact.

Having obtained the supersaturated solution of **3**, seeding experiments using the two types of seeds allowed us to demonstrate the distinct kinetics of terminal elongation and secondary nucleation-elongation (Figure 3a). Compared to the sigmoidal growth curve of the unseeded solution, a concave growth curve was observed for the helicoid-seeded solution, suggesting elongation at the active ends of the helicoid seed. AFM observation showed the formation of elongated helicoids, which further supports the terminal elongation (Figure 3b). In contrast, the accelerated sigmoidal growth curve was recorded for the toroid-seeded solution, illustrating the formation of new aggregates. Notably, AFM image showed randomly coiled fibers (Figure 3c). These observations demonstrate that toroid seed acts as active surface for secondary nucleation.
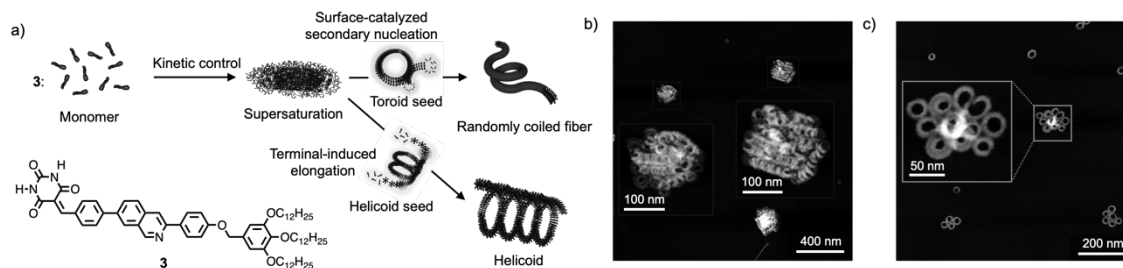

Figure 3. a) Schematic representation of supramolecular polymerization processes of **3** depending on seed topologies. b,c) AFM images of supramolecular polymers obtained by the helicoid-seeded (c) and toroid-seeded (d) solutions, respectively.

	4		1		0			
Datta Sougata								
71								
2022								

	Datta Sougata					
12 CSJ						
2022						

	Datta Sougata					
103						
2023						

Datta Sougata

A Tale of Celebration of 2020 Olympics in Chemistry in Japan!

12 CSJ

2022

O

(ITABASHI Hiroki)		
(YAGAI Shiki) (80344969)	(12501)	

O